



Proceedings  
of the 4th International Modelica Conference,  
Hamburg, March 7-8, 2005,  
Gerhard Schmitz (editor)

J. Eborn, H. Tummescheit, K. Prölb  
*Modelon AB, Sweden; TUHH, Germany*  
**AirConditioning - a Modelica Library for Dynamic Simulation of AC  
Systems**  
pp. 185-192

Paper presented at the 4th International Modelica Conference, March 7-8, 2005,  
Hamburg University of Technology, Hamburg-Harburg, Germany,  
organized by The Modelica Association and the Department of Thermodynamics, Hamburg University  
of Technology

All papers of this conference can be downloaded from  
<http://www.Modelica.org/events/Conference2005/>

#### Program Committee

- Prof. Gerhard Schmitz, Hamburg University of Technology, Germany (Program chair).
- Prof. Bernhard Bachmann, University of Applied Sciences Bielefeld, Germany.
- Dr. Francesco Casella, Politecnico di Milano, Italy.
- Dr. Hilding Elmqvist, Dynasim AB, Sweden.
- Prof. Peter Fritzson, University of Linkping, Sweden
- Prof. Martin Otter, DLR, Germany
- Dr. Michael Tiller, Ford Motor Company, USA
- Dr. Hubertus Tummescheit, Scynamics HB, Sweden

Local Organization: Gerhard Schmitz, Katrin Prölb, Wilson Casas, Henning Knigge, Jens Vassel, Stefan  
Wischhusen, TuTech Innovation GmbH

# AirConditioning – a Modelica Library for Dynamic Simulation of AC Systems

Hubertus Tummescheit<sup>†</sup> Jonas Eborn<sup>†</sup> Katrin Pröbß<sup>‡</sup>

<sup>†</sup> Modelon AB, Ideon Science Park, SE-223 70 Lund, Sweden

<sup>‡</sup> TU Hamburg–Harburg, Department of Thermodynamics, Denickestr. 17, D-21073 Hamburg, Germany

## Abstract

The AirConditioning library is a new, commercial Modelica library for the steady-state and transient simulation of air conditioning systems using modern, compact heat exchangers that use microchannel tubes instead of the bulkier fin-and-tube type heat exchangers. Currently it is mostly used by automotive OEMs and suppliers that need high-accuracy system level models to ensure both passenger comfort and energy efficiency of systems developed under the pressure of reduced design cycle times. The AirConditioning library contains basic correlations for heat and mass transfer and pressure drop, components for control volumes and flow resistances and advanced ready-to-use models for all relevant components of automotive air conditioning systems like condenser, evaporator, compressor, expansion devices and accumulator.

## 1 Introduction

The AirConditioning library has been derived from the Modelica library ThermoFluid [1, 2] and the ACLib library [11], with considerable enhancements in particular of the useability and robustness. Most of the fundamental design ideas outlined in [1, 2] are still valid, but a number of useability-oriented design improvements have been made also with respect to the specializations for AC-cycles described in [11]. Compared to ThermoFluid, also simplifications of the library structure have been made due to the reduced spectrum of applications. The most important differences are:

**Steady-state capabilities** Traditionally, AC system level models are only used as steady-state models, with the exception of very simplistic, often linear models for control design. ThermoFluid provided accurate dynamic models, but could not be used for steady-state tasks. AirConditioning bridges that gap and is suited both for

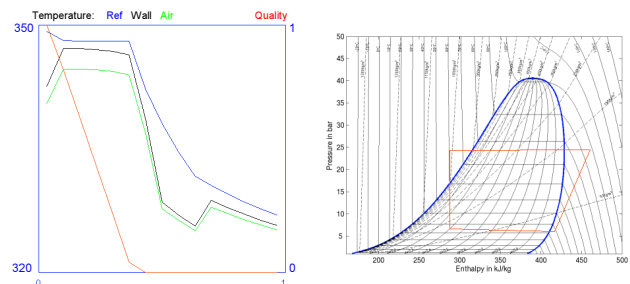


Figure 1: Examples of dynamic diagrams: spatial plot of condenser temperatures and ph-diagram for a R134a cycle.

dynamic and steady-state design computations, eliminating the need for multiple platforms and models. Significant improvements to the steady-state solvers in Dymola combined with model improvements have resulted in reliable steady-state initializations that can be used for design optimization.

**Re-designed user interface** The user interface improvements make full use of recent Dymola features: structured dialogs using hierarchy, tabs and groups where appropriate, illustrations linked into the dialogs for explanation of the parameter meaning and use of interactive elements for direct user feedback during simulation runs.

**Dynamic process diagrams** The UserInteraction library by Dynasim has been used to create dynamic interface elements for AC applications: spatial plots of temperatures or heat transfer coefficients and instantaneous corner points of the refrigerant cycle ph-diagram, as shown in Figure 1.

**New two-phase dynamic state model** The *integrated mean-density model* has been introduced for two-phase flow and greatly reduces the risk of discretization-triggered flow oscillations.

Apart from the robustness benefit it is also a reduced-order dynamic model that doesn't sacrifice accuracy, but rather allows the same or better accuracy with fewer dynamic states.

**Many AC component models** A number of new, specialized AC-component models have been added, e.g. internal heat exchanger, condenser with integrated receiver, short orifice tube, and many more.

**Compressor models** Two formulations for the compressor efficiencies have been developed: one is for the case of full-load measurement data only, reported in [4], the other computes also efficiencies for varying swash-plate angle inputs [3].

**Optional model encryption** Dynasim has developed a novel approach to model encryption that makes use of symbolic pre-processing of the model code before the actual encryption, called "scrambling". Most critical data is irretrievably removed from the model code even before proper encryption by evaluating all given parameters. The new method allows to selectively hide or reveal model features, giving the user full control over available model parameters and outputs. The symbolic evaluation of parameter expressions before code generation masks geometry information in a way that it is impossible to retrieve it even from the generated C-code.

### 1.1 Standard for model exchange

Dymola and the AirConditioning library was chosen by a group of German OEMs after a benchmark comparing it with other potential tools. During 2004, the tool was tested by the OEMs [9] and many of their suppliers, and then chosen as a common tool for model exchange between suppliers and OEMs. The benchmark and testing process has contributed to continued improvements of the library regarding the component-oriented requirements from suppliers and the system-oriented requirements of OEMs.

## 2 Heat exchanger models

In automotive refrigeration cycles heat is absorbed at the low temperature level of the cabin air or at ambient temperature and rejected at the discharge level of the ambient. For heat transfer between air and working fluid a condenser/gas cooler on the high pressure

level and an evaporator on the low pressure level are used, exploiting the low heat transfer resistance of the two-phase refrigerant. In some, mainly R744, applications, an internal refrigerant-to-refrigerant heat exchanger which transfers heat from one pressure level to the other enhances the performance of the cycle. Most heat exchanger types currently used in automotive air conditioning systems are represented by the library models or they can be developed from subcomponents.

### 2.1 Refrigerant side models

The fluid flow on the refrigerant side is based on dynamic control volume models that are different than the standard finite volume model found in ThermoFluid [1, 2]. The AirConditioning library uses from version 1.1 a new control volume that is similar to the one used in the ThermoPower library [5]. The main difference is that it is based on the computation of the *mean density*,  $\bar{\rho}$ , found by integrating over enthalpy along the flow, assuming constant pressure and taking into account the location of the phase boundaries ( $h_{pb}$ ),

$$\bar{\rho} = \int_{h_1}^{h_2} \rho(p, h) dh = \int_{h_1}^{h_{pb}} \rho(h) dh + \int_{h_{pb}}^{h_2} \rho(h) dh \quad (1)$$

With different inlet and outlet conditions and over the two boundaries,  $h_{liq}$  and  $h_{vap}$ , the integral splits up into 9 different cases, for which the analytic solution can be derived. In the one-phase region a regular mean value is used. Within the two-phase region the integral is rewritten using the expressions for quality  $x$  and volumity,  $v = 1/\rho$ , which are linear in enthalpy.

$$x = \frac{h - h_{liq}}{h_{vap} - h_{liq}} \quad v = x \cdot v_{vap} + (1 - x)v_{liq}$$

$$\int_{h_1}^{h_2} \rho(h) dh = \frac{h_{vap} - h_{liq}}{v_{vap} - v_{liq}} \int_{v_1}^{v_2} \frac{1}{v} dv = \frac{h_{vap} - h_{liq}}{v_{vap} - v_{liq}} \ln \frac{v_2}{v_1}$$

The expressions are such that they are continuously differentiable even across the phase boundaries. The analytic derivatives of the mean density w.r.t. the inputs of the fluid property calculation have also been derived and validated using the new automatic differentiation feature of Dymola [6].

Due to the magnitudes of temperature gradients and pressure drops, a different parameterization than chosen by [5] has to be implemented for air conditioning systems: pressure drops have a larger influence on the driving temperature difference and can not be neglected. Another important feature of the refrigerant side models is to fully make use of the fact that

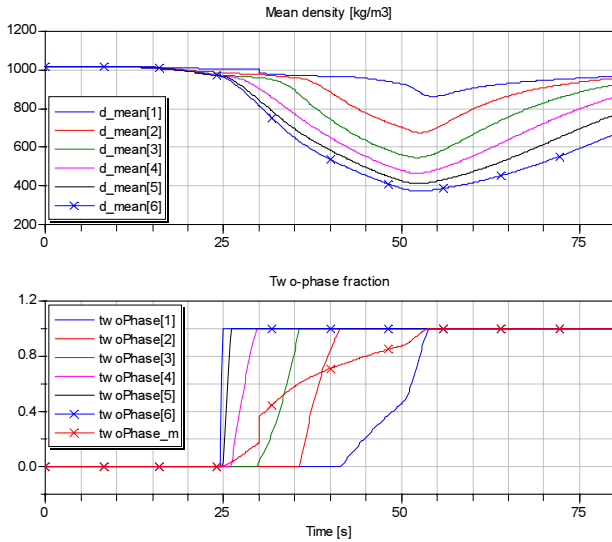


Figure 2: Mean density and two-phase fraction in a six segment pipe with R134a during a rapid transient starting in all liquid phase. Both properties are smooth throughout the simulation, with the exception of  $d_{mean}[1]$  and the overall two-phase fraction,  $twoPhase_m$ , that jump when the inlet enthalpy changes at  $t=30s$ .

the phase boundary location is resolved continuously within each finite volume and not just discretely for each volume. Using the two-phase length fraction for interpolation of all phase dependent correlations and properties improves calculation accuracy vastly. An added benefit is that the interpolation also makes variables such as heat transfer coefficient change continuously with time when the phase boundary moves from one finite volume to the next.

The smooth results of the mean density model is illustrated in Figure 2 where the calculated mean density and two-phase fraction of a refrigerant pipe is shown. Heat transfer properties are interpolated with the individual two-phase fraction of each volume, while the pressure loss model can use the overall two-phase fraction of the pipe. The pipe model with  $n = 6$  will then only have one dynamic pressure state but six enthalpy states. This model is normally used for the refrigerant side of a heat exchanger, where a six pass evaporator with  $n = 3$  will have six pressure states and eighteen enthalpy states.

## 2.2 Air side models

Air side models in compact heat exchangers of air conditioning systems are characterized by three features:

- sharp gradients along short flow paths,

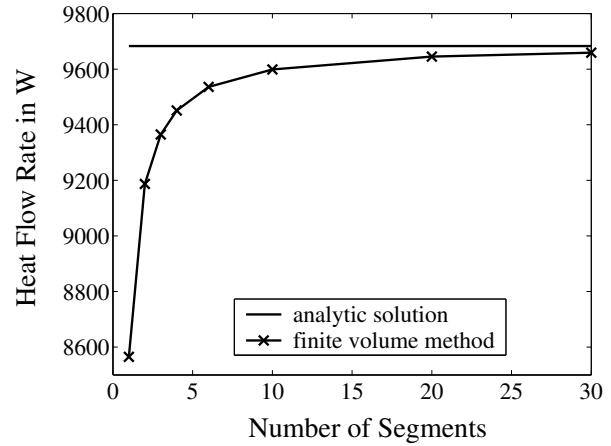


Figure 3: Influence of air side discretization on total transferred heat in a refrigerant condenser

- discontinuous phenomena depending on condensing/ non-condensing conditions on cold surfaces and
- very short residence times of an air particle inside the heat exchanger.

To accommodate for these features, two different models have been developed for the air side of compact automotive heat exchangers. One is a discretized finite volume based model with steady-state mass- and energy balances for each volume, the other is a symbolic solution of the outflow temperature found by applying constant medium properties along the flow path. In both cases the correlation for convective heat transfer is used,

$$\dot{Q} = \alpha A (T_{wall} - T)$$

where  $\dot{Q}$  is the heat flow rate,  $\alpha$  is the coefficient of heat transfer,  $A$  is the surface area,  $T$  and  $T_{wall}$  are the temperature in the bulk flow and at the wall surface, respectively. The heat connector variables  $\dot{Q}$  and  $T_{wall}$  provide an interface to wall models. The computational burden of dynamic balances with an increased number of dynamic states is avoided by using steady-state balances, which is justified by the short residence time of the fluid.

Due to the sharp gradients and/or discontinuities on the air side, the finite volume method requires a relatively high discretization. If high accuracy is required, typically 10 – 15 elements are needed for the air passage<sup>1</sup> Figure 3 shows simulation results for the steady-state heat flow rate of a compact flat tube condenser of 2

<sup>1</sup>For multi-layered heat exchangers this includes the sum of elements for all layers, (air segments/layer)\*(number of layers).

cm depth comparing the finite volume and the analytical approach. Air temperatures at inlet and outlet were 320 K and around 336 K, respectively.

A symbolic solution for the outlet state can only be found if the water content of the air remains constant along the flow path, which is only the case for very low or zero inlet humidities or air heating. In the finite volume model, when the wall surface temperature drops below the saturation temperature of the bulk flow, the amount of condensing humidity will be determined by applying a heat and mass transfer analogy approach. Assuming a similarity in the shape of the temperature boundary layer of a convective fluid flow and that of the respective concentration boundary layer, the mass transfer coefficient  $\beta$  can be determined from

$$\beta = \frac{Le^{(m-1)}\alpha}{\rho c_p}$$

where  $Le$  is the Lewis number,  $\alpha$  the coefficient of heat transfer and with  $m = 1/3$  valid for most applications [12]. The driving potential of water condensation is then formed by the water content in the bulk flow  $X$  and that for saturation at surface temperature  $X_{sat}(T_{wall})$ . Assuming the ideal gas law applies, the condensate flow rate  $\dot{m}_w$  is computed from

$$\dot{m}_w = \beta \rho A (X - X_{sat}(T_{wall}))$$

with  $\rho$  as the bulk flow density. The model allows outlet humidities below 100% and water condensation at the same time. The correct determination of the latent heat is important, as it can make up around 50% of the total transferred heat.

Heat transfer and pressure drop correlations for air side specific geometries from the literature are part of the library. Additional user correlations can be incorporated on the component top level by using replaceable classes.

### 2.3 Air-refrigerant heat exchangers

Condensers/gas coolers and evaporators in automotive refrigeration cycles are mostly of cross, cross-co or cross-counter flow type and consist of louvered fins and extruded microchannel flat tubes, both made of aluminium, as schematically shown in Figure 4a). The models in the library are composed of refrigerant and air cross flow elements with walls between the two media [11]. Heat conduction in the solid material in fluid flow direction is neglected. The dynamic behavior of the component is mainly influenced by the amount and distribution of the solid wall material and

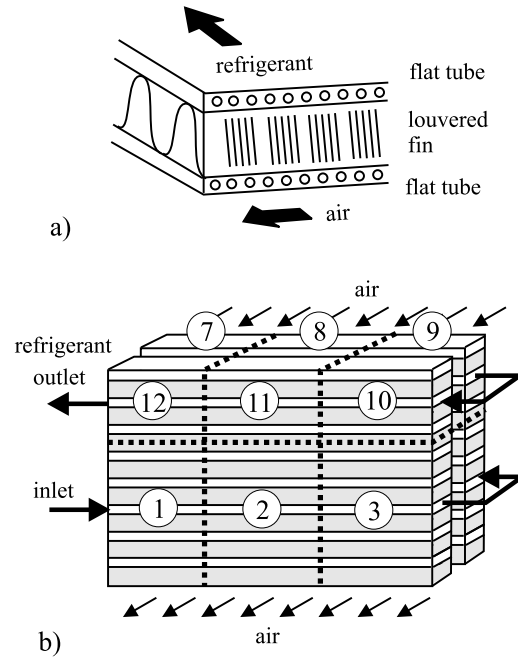


Figure 4: a) cross flow of air and refrigerant, b) 4-pass condenser with horizontal refrigerant flow and a refrigerant side discretization of 3 per pass

associated heat capacity. On both sides of the wall, several parallel flow channels are lumped into one homogeneous flow for efficiency reasons. The refrigerant path through the component is treated as one pipe flow with variable cross section and one air element associated with each flow segment. Each air element is further discretized or symbolically integrated along its flow. Automatic coupling of air elements is made according to the parameter-specified and component type dependent 3D orientation, e.g. as the evaporator shown in Figure 6 and to the user defined segmentation of the refrigerant flow. Both parameters are merged into a 3D-matrix, which defines the position of each refrigerant segment with respect to a fixed coordinate system. The condenser in Figure 4b) would yield a 2 by 2 by 3 matrix which is used for conditional connect statements of air inlets and outlets in the component. This approach allows for a wide variety of flow paths and a 2D-interface for inhomogeneous air inlet. However, the interface resolution is directly coupled to the number of refrigerant passes through the heat exchanger and their segmentation.

### 2.4 Internal heat exchangers

For systems using the refrigerant R744 (CO<sub>2</sub>) as the cycle fluid, it is quite common to have an internal heat exchanger between the high pressure side, after the

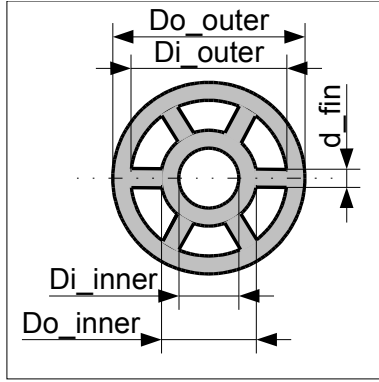


Figure 5: Cross section of tube-in-tube internal heat exchanger.

gascooler, and the low pressure side, between the accumulator and the compressor. The base classes for the internal heat exchanger are identical to those for the refrigerant side of flat tube heat exchangers.

Currently used internal heat exchangers come in a wide variety of geometries. Tube-in-tube type internal heat exchangers as in Figure 5 can be parametrized directly from the geometrical data. For other types of internal heat exchangers, the user has to compute parameters like the hydraulic diameter and the heat transfer areas by hand.

### 3 Swash plate compressor model

The compressor is modeled as a steady-state map that relates suction- and discharge states and mass flow. Due to the wide variety of mechanical constructions, a simple parameterization of a swash-plate or swashing compressor has to be based on an extensive set of measurements. The measurements are used to adapt the free parameters of efficiency functions that are chosen to have physically reasonable asymptotics for high pressure ratios and low rotational speed. The form of the functions is similar to the one presented in [4], and varies slightly for different compressor types. The compressor model uses three functions to characterize the compressor efficiencies, the volumetric efficiency  $\lambda_{eff}$ , the effective isentropic efficiency  $\eta_{eff}$  and the isentropic efficiency  $\eta_{is}$ . The efficiencies are defined as

$$\begin{aligned}\lambda_{eff} &= \frac{\dot{m}_{eff}}{Vn\rho(p_s, T_s)} \\ \eta_{eff} &= \frac{P_{is}}{P_{eff}} = \frac{(h_{d,is} - h_s)\dot{m}_{eff}}{2\pi|M|n} \\ \eta_{is} &= \frac{h_{d,is} - h_s}{h_d - h_s}\end{aligned}$$

In the definitions above,  $p$  is the pressure,  $T$  temperature,  $V$  displacement volume,  $\rho$  density,  $h$  specific enthalpy,  $P$  power,  $\dot{m}$  mass flow and  $M$  the torque of the compressor. In the subscripts  $d$  refers to the discharge side,  $s$  to the suction side,  $is$  to isentropic conditions and  $eff$  to effective values.

In order to simplify the situation in early development stages, the efficiency functions are factored into two parts: one that captures the influence of the pressure ratio and rotational speed,  $f(\pi, n)$  and another one that takes into account the control of the swash plate angle and rotational speed,  $g(x, n)$ . Measurements of the influence of the swash plate angle are not always available, and due to this separation it is still possible to derive efficiencies for the full load case. A typical form of the efficiency functions is given below.

$$\lambda_{eff} = \left( \pi_0 - \frac{p_d/p_s}{\pi_0 - 1} \right)^2 \left( \frac{x - x_0}{1 - x_0} \right) (a_2 n^2 x + a_1 n x + a_0)$$

$$\eta_{is} = f(\pi, n) \cdot g(x, n)$$

$$f(\pi, n) = a \frac{\pi_0 - \pi}{\pi_0} - ab \left( \frac{1}{b} \frac{\pi_0 - 1}{\pi_0} \right)^\pi$$

$$g(x, n) = \left( 1 - \left( \frac{x - 1}{x_0 - 1} \right)^k (c + 1 - b)x \right)$$

$$a = a(n) = a_1 n + a_0$$

$$b = b(n) = b_3 n^3 + b_2 n^2 + b_1 n + b_0$$

$$c = c(n) = c_1 n + c_0$$

$$k = k(n) = k_1 n + k_0$$

The effective isentropic efficiency has the same functional form as the isentropic efficiency. Two of the constants have physical significance,  $\pi_0$  is the upper limit of the pressure ratio at which the discharge mass flow decreases to 0. Similarly,  $x_0$  is the lower limit of the relative displacement control signal where the compressor does not discharge any more. The parameters  $a_i$ ,  $b_i$ ,  $c_i$  and  $k_i$  are free parameters that have to be adapted to measurement data.

### 4 Expansion devices and valves

The library includes simple orifice and thermostatic expansion valve (TXV) models. Several models of these short flow restrictions are based on the computation of mass flow of compressible fluids as described in DIN EN 60543-2-1, computing a flow coefficient  $K_v$  in  $\text{m}^3/\text{h}$ . The model takes into account the choking of flow above the critical pressure ratio. Simpler models

with a constant  $\zeta$ -parameter,

$$\Delta p = \frac{|\dot{m}| \dot{m} \zeta}{2A^2 \rho}$$

and with quadratic scaling based on nominal parameters are also available. The TXV is based on the DIN valve model, with a PI-controller with a suitable time constant representing the bulb dynamics.

### 4.1 Short orifice tube

A geometrical model of a short orifice tube is also included according to the correlation in [7]. The orifice tube model has been validated against measured data from the reference with good results over a wide range of operating conditions. The mass flow error is less than 5-10% in all but extreme cases. For sub-cooled conditions the liquid flow equation 2 is used, and for fully choked flow equations 3-4 are used. Inbetween these extremes the mass flow is interpolated based on upstream quality.

$$\dot{m}_l = C_1 D_{tube}^2 \sqrt{2\rho_l(p_1 - p_f)} \quad (2)$$

$$\dot{m}_c = \frac{\pi}{4} p_1 D_{tube}^2 \sqrt{\frac{M^2 \kappa}{RT}} \quad (3)$$

$$\lambda \frac{L_{tube}}{D_{tube}} = \frac{1 - M^2}{\kappa M^2} + \frac{\kappa + 1}{2\kappa} \log \frac{M^2(\kappa + 1)}{2(1 + \frac{\kappa - 1}{2M^2})} \quad (4)$$

In the equations above  $\lambda$  is the friction coefficient,  $\kappa$  is the ratio of specific heats and  $p_1$  is upstream pressure. The adjusted downstream pressure,  $p_f$ , depends on subcooling temperature, critical pressure and tube dimensions [8]. Note that Equation 4 is an implicit equation for the Mach number  $M$ . It is used exactly as quoted in the orifice tube model.

## 5 User interface

The library makes full use of recent Dymola features to make the models easy to use. Component parameter dialogs are structured using tabs and grouping, with appropriate text and graphical explanations. All non-numerical input values can be selected from drop-down menus and the lists of choices for correlation models and geometry records are automatically updated using the annotation *choicesAllMatching*. As an example, the geometry parameter dialog for a flat tube evaporator is shown in Figure 6.

To further enable an easy understanding of simulation results, dynamic diagrams have been integrated into

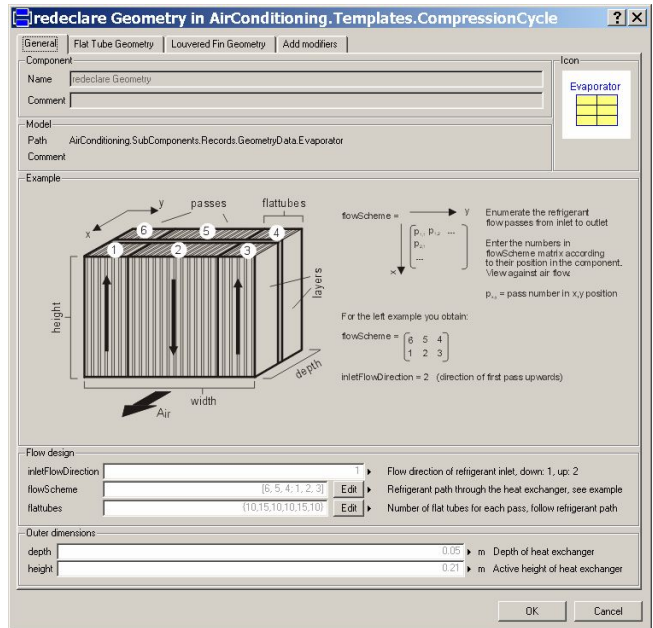


Figure 6: Parameter dialog for specifying evaporator geometry parameters. Illustrations and explanations provide help for the input fields and different parameters are grouped under tabs; General, Flat tube geometry and Louvered fin geometry.

example models using the library UserInteraction. Dynamic components include value displays showing e.g. instantaneous temperature and transferred heat, spatial plots showing temperatures, quality or other properties along the refrigerant flow direction and ph-diagrams that illustrate the full refrigerant cycle behavior. Examples of dynamic diagrams are shown in Figure 1.

## 6 Initialization

Robust steady-state initialization is critical for using dynamic AC models also for steady-state applications and system design optimization. From a tool and library implementation viewpoint all of the pieces below are important to allow robust initialization.

- Reduce the number of required input parameters for initialization for distributed parameter systems, but still achieve convergence for reasonable input values. This has to be done in the library design, and it often requires that *template*<sup>2</sup> models are provided that reduce inputs for specific configurations, including the boundary conditions.

<sup>2</sup>These are example models tailored for different applications in AirConditioning.

n_ref	2	4	6	10
total variables	11132	21992	32852	54572
dynamic states	38	74	110	182
iteration vars	301	601	901	1501
Init time [s]	3.3	13.8	34.4	113

Table 1: Steady-state initialization times for different discretizations of a six pass evaporator testbench from AirConditioning 1.0 using Dymola 5.3b.

The remaining parameters should be those that are typically measured for the device.

- Improvements of solver robustness in the simulation tool. Dymola recently introduced two new features: a global homotopy method for the solution of large systems and much improved handling for scalar systems. Due to the tearing technique, scalar systems are much more frequent than would be expected otherwise.
- Be aware of particular problem cases in the model equations and avoid them or rewrite them in a way that is numerically easier to handle.

Using all these techniques, initialization problems with thousands of iteration variables are possible to solve with the current Dymola version. Results from a computation benchmark are shown in Table 1.<sup>3</sup> An open point for even larger equation systems is to use sparse methods also after symbolically tearing and reducing the size of initial equation systems.

## 7 Model encryption

To securely exchange accurate first principle based simulation models without revealing proprietary data to third party users, a careful balance has to be found between two conflicting requirements:

- If the model information is completely hidden, the model is similar to a black-box model and will often not be of much use to the end user.
- If too many model details are revealed, many others can be reconstructed with little effort.

*Encrypted save total* models in Dymola keep only the connector variables, top-level parameters and outputs visible to a user. By default, the new encryption method hides as much data as is possible. If users

<sup>3</sup>The benchmark was performed on a 3.2 GHz Pentium 4 with 512 MB memory.

require additional input parameters or outputs, these have to be propagated explicitly to the top level by the owner that exports the model and makes it available. The method *Encrypted save total* consists of two distinct phases:

1. First, the model is pre-processed in a step called *scrambling*, which flattens the model (removes the composition hierarchy), evaluates all expressions in the model that can be evaluated, and changes all variable names in the model to generic ones. The evaluation of parameters removes most sensitive parameters completely from the model.
2. In a second step, the scrambled model is also encrypted. In the user interface, the encrypted model shows only the information needed to use and run the model; connectors and public, top-level parameters.

The unique advantage of the new encryption method is that sensitive information is irretrievably removed from the model in many cases. Consider e.g. the computation of a volume from parameters width, length and height:  $V = w * l * h$ . After scrambling, only the value for  $V$  remains in the scrambled code. Obviously it is impossible to back-calculate the original parameters from this information.

## 8 Transient simulation of automotive systems

In the past, the influence of AC-systems on fuel consumption has been neglected by legislative bodies and automotive manufacturers. This situation is currently changing, and accurate fuel consumption estimates are needed also for the case of a running AC unit. Figure 7 shows some of the key system parameters when running a New European Driving Cycle (NEDC) that contains an urban as well as an extra-urban section. In [9], more results from simulating driving cycles using the AirConditioning library are presented. Models from AirConditioning can be coupled directly to the PowerTrain Modelica library [10] for fuel consumption calculation.

## 9 Summary

AirConditioning is a comprehensive Modelica library for the simulation of automotive air conditioning systems. AirConditioning contains models for current,

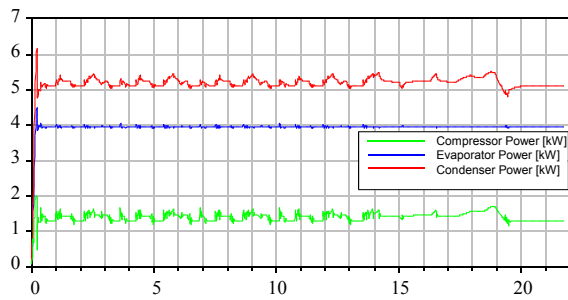


Figure 7: AC-system key parameters during NEDC driving cycle. Condenser power is the top line, compressor power the bottom line.

R134a based systems as well as systems under development using R744. It has been chosen by a group of automotive OEM and suppliers as a standardized tool for exchanging models for automotive AC-systems. Dynasim AB has added a new encryption method to accommodate the exchange of models containing proprietary data. The refrigerant and air side models have been adapted to cover the accuracy needed for component simulation and the flexibility and speed needed for system simulation. AC components and systems can be simulated in steady-state and dynamic conditions, and the models can be coupled to other Modelica libraries, e.g. for powertrain models.

## References

[1] Eborn, J. *On Model Libraries for Thermo-hydraulic Applications*. Ph.D. thesis TFRT-1061-SE, Dept of Automatic Control, Lund Inst. of Technology, Lund, Sweden, 2001.

[2] Tummescheit, H. *Design and Implementation of Object-Oriented Model Libraries using Modelica*. Ph.D. thesis TFRT-1063-SE, Dept of Automatic Control, Lund Inst. of Technology, Lund, Sweden, 2002.

[3] Försterling, S. Personal communication, 2004.

[4] Försterling, S. *Vergleichende Untersuchung von CO<sub>2</sub>-Verdichtern in Hinblick auf den Einsatz in mobilen Anwendungen*, Ph.D. thesis, TU Braunschweig, 2004.

[5] Casella, F. and Leva, A. Modelica open library for power plant simulation: design and experimental validation, In *Proc. of 3rd International Modelica Conference*, Linköping, Sweden, 2003.

[6] Olsson, H., Elmqvist, H. and Tummescheit, H. Using Automatic Differentiation for Partial Derivatives

of Functions in Modelica, In *Proceedings of the 4th International Modelica Conference*, Hamburg, 2005.

[7] Singh, G.M., Hrnjak, P.S. and Bullard, C.W. Flow of Refrigerant R134a through Orifice Tubes, *HVAC & Refrigeration Research*, 7:3, pp. 245–262, July 2001.

[8] Kim, Y. and O’Neal, D.L. A Semi-Empirical Model of Two-Phase Flow of Refrigerant-134a through Short Orifice Tubes, *Experimental & Thermal Fluid Science*, 9:4, pp. 426–435, 1994.

[9] Limperich, D., Braun, M., Schmitz, G. and Prölb, K. System Simulation of Automotive Refrigeration Cycles, In *Proceedings of the 4th International Modelica Conference*, Hamburg, 2005.

[10] Dynasim AB, <http://www.dynasim.se/models.htm>, Accessed January 2005.

[11] Pfafferott, T., *Dynamische Simulation von CO<sub>2</sub> Kälteprozessen*, Ph.D. thesis, Department of Thermodynamics, TU Hamburg-Harburg. In *Berichte aus der Thermodynamik*, Shaker-Verlag, Aachen, 2005.

[12] Incropera, F.P. and DeWitt, D.P. *Fundamentals of Heat and Mass Transfer*, Wiley & Sons, 5th ed., New York, 2002.